Wheat *VRN1* and *FUL2* play critical and redundant roles in spikelet meristem identity and spike determinacy

Chengxia Li[1, 2*], Huiqiong Lin[1, 2*], Andrew Chen[1, 3], Meiyee Lau[1], Judy Jernstedt[1] and Jorge Dubcovsky[1, 2‡]

[*] These authors contributed equally to this work

[1]Department of Plant Sciences, University of California, Davis, CA 95616, USA.

[2]Howard Hughes Medical Institute, Chevy Chase, MD 20815, USA.

[3]Current address: University of Queensland, Brisbane, QLD4072, Australia

[‡] Author for correspondence: jdubcovsky@ucdavis.edu. Phone: 530 752 5159

Running title: Spikelet meristem identity genes

Key words: wheat, spike development, spikelet, meristem identity, MADS-box,

Word count: 6190

SUMMARY STATEMENT

The wheat MADS-box proteins VRN1 and FUL2 play critical and overlapping roles in the development of spikelets, which are the basic unit of all grass inflorescences.

ABSTRACT

The spikelet is the basic unit of the grass inflorescence. In this study, we show that wheat MADS-box genes *VRN1* and *FUL2* play critical and redundant roles in the determination of spikelet meristem identity. Combined loss-of-function mutations of these two genes (*vrn1ful2*-null) were sufficient to revert lateral spikelet meristems into vegetative meristems in the spikes of tetraploid wheat. These plants were also unable to form a terminal spikelet and had an indeterminate inflorescence. The single *vrn1*-null and *ful2*-null mutants showed increased number of spikelets per spike, likely due to a delayed formation of the terminal spikelet. Mutations in these two genes and in the more distantly related paralog *FUL3*, also affected wheat heading time and stem elongation. The *ful2*-null mutant also showed a higher number of florets per spikelet, which together with a higher number of spikelets, resulted in a significant increase in the number of grains per spike in the field. Our results suggest that a better understanding of the basic mechanisms underlying wheat spike development can inform future strategies to improve grain yield in wheat.

INTRODUCTION

The grass family (Poaceae) has approximately 10,000 species, including important food crops such as rice, maize, sorghum, barley, and wheat (Kellogg, 2001). The flowers of these species are organized in a unique and diagnostic structure called spikelet (literally "little spike"), which is a compact and indeterminate branching inflorescence developing within the larger inflorescence (Malcomber et al., 2006). A spikelet typically has two sterile bracts (called glumes) enclosing one or more florets. Each floret includes a carpel, 3 or 6 stamens and two modified petals (called lodicules) subtended by two bract-like organs, the palea and the lemma (Preston et al., 2009).

The spikelet adds a recursive level of complexity to grass inflorescences, in which different types of meristems are responsible for a large diversity of inflorescence architectures (Ciaffi et al., 2011). Development of the ancestral grass inflorescence, the panicle, begins when the shoot apical meristem (SAM) changes from a vegetative meristem (VM) that produces leaves to an inflorescence meristem (IM), which elongates and generates lateral primary branch meristems (PBMs). The PBMs generate secondary branches as axillary meristems (SBM), and both PBMs and SBMs terminate into spikelet meristems (SMs), resulting in a highly branched structure. The SMs then generate glumes and lateral floral meristems (FMs), which vary in number across grass species (Malcomber et al., 2006).

In wheat, a drastic shortening of the lateral branches results in sessile spikelets attached directly to the central axis or rachis and the formation of a derived inflorescence, a spike, in which the spikelets are arranged alternately in opposite vertical rows (a distichous pattern) (Kellogg et al., 2013). In the initial stage of wheat spike development, the IM generates a double-ridge structure in which the lower ridges arrest, while the upper ridges acquire SM identity and form spikelets. The number of spikelets per spike is determined by the number of lateral meristems formed before the transition of the IM into a SM to form the terminal spikelet. Although the growth of the wheat spike is determinate, the growth of each spikelet is indeterminate, with each SM initiating a variable number of FMs (Ciaffi et al., 2011). The numbers of spikelets per spike and florets per spikelet determine the maximum number of grains per spike and are, therefore, important components of wheat grain yield potential.

Studies in Arabidopsis, which has a simpler inflorescence than grasses (Malcomber et al., 2006), have shown that MIKC-type MADS-box transcription factors *APETALA1* (*AP1),* *CAULIFLOWER* (*CAL*) and *FRUITFULL* (*FUL*) are prominent players in the determination of floral meristem identity. In the triple *ap1calful* mutant, the IM is not able to produce flowers and reiterates the development of leafy shoots (Ferrándiz et al., 2000). MIKC-type MADS-box proteins have a highly conserved MADS DNA-binding domain (also important for dimerization and nuclear localization), an Intervening (I) domain, a Keratin-like (K) domain critical for dimerization and multimeric complex formation, and a C-terminal domain involved in transcriptional activation. These proteins bind as dimers to DNA sequences named 'CArG' boxes, and can organize in tetrameric complexes that can recognize different CArG boxes. The multimeric nature of these complexes generates a large number of combinatorial possibilities with different targets and functions (Honma and Goto, 2001; Theissen et al., 2016).

The closest homologs to the Arabidopsis MADS-box genes *AP1*, *CAL* and *FUL* in the grass lineage are *VERNALIZATION 1* (*VRN1*), *FUL2* and *FUL3*. A phylogenetic analysis of the proteins encoded by these genes indicates that these Arabidopsis and grass groups have independent subfunctionalization stories (Preston and Kellogg, 2006) and Fig. S1). In the grass lineage, a duplication that occurred close to the divergence between monocots and eudicots resulted in the separation of the *FUL3* clade. A later duplication that occurred near the base of the radiation of the grasses resulted in the *VRN1* and *FUL2* clades (Preston and Kellogg, 2006). Large truncation mutations in the two *VRN1* homeologs in tetraploid wheat delay heading time, but do not alter spikelet morphology or the ability of flowers to form viable grains (Chen and Dubcovsky, 2012). Since *FUL2* and *FUL3* are the closest paralogs of *VRN1*, we hypothesized that they could have redundant spikelet and floral meristem identity functions.

In this study, we generated truncation mutants for the two homeologs of both *FUL2* and *FUL3* in the same tetraploid background carrying the *vrn1* truncation mutations and intercrossed them to generate double- and triple-null mutants. Characterization of these mutants revealed that *VRN1*, *FUL2* and *FUL3* have overlapping roles in the regulation of flowering time and stem elongation and, more importantly, that *VRN1* and *FUL2* (but not *FUL3*) are critical and redundant in the determination of spikelet meristem identity and spike determinacy. Individual *vrn1* and *ful2* truncation mutants showed significant increases in the number of spikelets and grains per spike,

94 suggesting that manipulations of these genes may contribute to increasing wheat grain yield
95 potential.

96

97 **RESULTS**

98 **Mutations of *FUL2* and *FUL3* affect stem elongation**

99 We identified loss-of-function mutations in the A and B genome homeologs of *FUL2* and *FUL3*
100 (Fig. S2) in an EMS-mutagenized population of the tetraploid spring wheat variety Kronos
101 (Krasileva et al., 2017; Uauy et al., 2009) and backcrossed each individual mutant two to three
102 times to Kronos to reduce background mutations. Then, we intercrossed the A and B genome
103 homeologs for each gene and selected plants homozygous for both mutations. For simplicity,
104 mutants with large truncation mutations in both homeologs will hereafter be referred to as null
105 mutants (e.g. *vrn1*-null). The *ful2*-null and *ful3*-null mutants were crossed with *vrn1*-null (Chen
106 and Dubcovsky, 2012) to generate *vrn1ful2*-null and *vrn1ful3*-null mutants, which were
107 intercrossed to generate the *vrn1ful2ful3*-null mutant (Fig. S2). The wild type Kronos carries a
108 functional *VERNALIZATION 2* (*VRN2*) flowering repressor, which results in extremely late
109 flowering in the presence of the *vrn1*-null mutation (Chen and Dubcovsky, 2012). To avoid this
110 problem all mutants described in this study were developed in a Kronos *vrn2*-null background
111 (Distelfeld et al., 2009), unless indicated otherwise. This line is referred to in figures as the
112 control line.

113 Since some mutant combinations lack real spikes, we decided to determine final stem length
114 from the base of the plant to the base of the spike instead of total plant height. The individual
115 *ful3*-null and *vrn1*-null mutants showed marginal or not significant reductions in stem length (5
116 % and 3 %, respectively, Fig. S3A). However, a factorial experiment including all four *VRN1* by
117 *FUL3* wild type and null allele combinations, revealed highly significant effects for both genes
118 ($P = 0.002$) and a significant synergistic interaction ($P = 0.019$) that resulted in a 17 % reduction
119 in stem length in the *vrn1ful3*-null mutant (Fig. S3B). The stems of plants carrying only the *ful2*-
120 null mutation were 27% shorter than the control ($P < 0.0001$, Fig. S3C) and the differences were
121 magnified in the double-null (*vrn1ful2*-null, 40% reduction, $P < 0.0001$, Fig. S3D) and triple-
122 null mutants (*vrn1ful2ful3*-null, 63% reduction, $P < 0.0001$, Fig. S3E). Taken together, these
123 results suggest that *VRN1*, *FUL2* and *FUL3* have redundant roles in the regulation of stem

elongation, and that the effect of the individual genes is larger in the absence of the other paralogs.

FUL2 and *FUL3* affect flowering and heading time

Functional redundancy among *VRN1*, *FUL2* and *FUL3* was also observed for heading time, but the effect of the latter two genes was detected only in the absence of *VRN1*. The *vrn1*-null mutant headed 37.5 d later than the control (Fig. 1A), but the differences in heading time for the *ful2*-null (Fig. 1B), *ful3*-null and *ful2ful3*-null mutants in the presence of the strong *Vrn-A1* allele were non-significant (Fig. 1C). For the *vrn1ful2*-null and *vrn1ful2ful3*-null mutants, it was not possible to determine heading times accurately because they have short stems and abnormal spikes that interfere with normal ear emergence. To study the effect of these mutations on flowering time we determined instead the timing of the transition between vegetative and double-ridge stages (Fig. 1D). The SAM in *vrn1*-null and *vrn1vrn3*-null transitioned to the double-ridge stage around 31 days, but this transition was delayed 3-6 d in *vrn1ful2*-null and 9 to 12 d in *vrn1ful2ful3*-null (Fig. 1D). The latter result indicates that *FUL3* has a residual ability to accelerate flowering time in the absence of *VRN1* and *FUL2*.

Transgenic Kronos plants overexpressing the coding regions of *FUL2* fused with a C-terminal 3xHA tag (henceforth *Ubi::FUL2*, Fig. 1E, events #1 and #6) or *FUL3* fused with a C-terminal 4xMYC tag (henceforth *Ubi::FUL3*, Fig. 1F, events #4 and #5) headed two to four days earlier than the non-transgenic sister lines ($P < 0.0001$). The effect of *Ubi::FUL2* on heading time was further characterized in the presence of different *VRN1* and *VRN2* alleles in the F_2 progeny from the cross between *Ubi::FUL2* (*Vrn1Vrn2*) and *vrn1vrn2*-null under greenhouse conditions. Using a three-way factorial ANOVA, we detected highly significant effects in heading time for each gene and for all two- and three-way interactions ($P < 0.0001$, Table S3). As an example of these interactions, the differences in heading time between the *FUL2*-wt and *Ubi::FUL2* alleles in the presence of a functional *VRN2* allele were small in lines homozygous for the functional *VRN1* allele (2.6 d, Fig. 1E), intermediate in *VRN1* heterozygous lines (11.1 d, Fig. 1G) and large in homozygous *vrn1*-null mutants (53 d, Fig. 1H). These results indicate that the effect of the *Ubi::FUL2* transgene on heading time depends on the particular *VRN1* and *VRN2* alleles present in the genetic background (Fig. G-H).

153 In summary, the strong effect of *VRN1* in the acceleration of wheat flowering time can mask the
154 smaller effects of *FUL2* and *FUL3*, but in the absence of *VRN1*, both *FUL2* and *FUL3* have
155 redundant effects on accelerating wheat flowering time.

156 **_FUL2_ and _VRN1_ play critical but redundant roles in the determination of spikelet**
157 **meristem identity**

158 The *vrn1*-null and *ful2*-null individual mutants showed normal spikelets and flowers (Fig. 2A-E),
159 but the plants carrying both mutations showed striking developmental changes. The *vrn1ful2*-null
160 mutants had a spike-like structure (Fig. 2A) in which all the lateral spikelets were replaced by
161 leafy shoots. These shoots produced normal leaves and most of them had no floral organs (Fig.
162 2F-G). However, dissection of tillers located in the basal part of this spike-like structure revealed
163 that some of them had leafy bracts subtending abnormal floral organs in the expected position of
164 the first floret (Fig. S4A-E). Floral abnormalities included leafy lodicules, reduced number of
165 anthers or anthers fused to ovaries and multiple ovaries (Fig. S4C-E). Dissection and Scanning
166 Electron-Microscopy (SEM) images of the *vrn1*-null and *vrn1ful2*-null IM showed lateral
167 meristems organized in a distichous phyllotaxis in both mutants (Fig. 2D and H). However,
168 while these lateral meristems progressed to SMs that formed normal glume flower primordia in
169 the *vrn1*-null and *vrn1ful3*-null mutants (Fig. 2D-E), they reverted to VMs generating leaf
170 primordia in the *vrn1ful2*-null mutant (Fig. 2H-I). After producing a variable number of leaves,
171 those lateral VMs transitioned again to IMs that generated their own lateral VMs (Fig. S4A-B).

172 The *vrn1ful2ful3*-null mutant showed a similar spike-like structure as the *vrn1ful2*-null mutant,
173 with vegetative meristems replacing the lateral spikelet meristems and vegetative shoots
174 replacing the spikelets (Fig. 2J-K). Compared with the *vrn1ful2*-null mutant, the stems in the
175 triple-null mutants were shorter and frequently had difficulty emerging from leaf sheaths,
176 resulting in smaller spike-like structures with curly leaves (Fig. 2A and J). Both *vrn1ful3*-null
177 and *ful2ful3*-null plants showed normal spikelets and fertile flowers. Since *FUL3* played a
178 limited role in the determination of the SM identity, we focused subsequent studies on the
179 *vrn1ful2*-null mutant.

180 To compare the relative roles of *VRN1* and *FUL2* on SM identity, we examined their individual
181 ability to restore fertile flowers when present as a single functional copy in a heterozygous state
182 (underlined). Both *ful2*-null/*Vrn-A1* *vrn-B1-null* (functional *Vrn1* allele for spring growth habit)

and *ful2*-null/*vrn-A1-null* *vrn-B1* (functional *vrn1* allele for winter growth habit) produced spike-like structures with leafy lateral shoots (Fig. 3A-B) and normal floral organs (Fig. 3C) but no viable seeds. The developing spikes of these plants showed lateral meristems with floral primordia (Fig. 3D), some of which later showed elongated rachillas and leafy organs (Fig. 3E-G). By contrast, the presence of a single heterozygous copy of *FUL2* in a *vrn1*-null background (*vrn1*-null/*ful2-A* *Ful2-B*) resulted in spikelets that were less leafy than the previous mutants (Fig. 3H). Some of these spikelets were more similar to the control and were able to set some viable seeds. Abnormal spikelets (Fig. 3I) and basal branches with lateral spikelets and fertile florets (Fig. 3J) were also observed in this mutant. Taken together, these results indicate that *VRN1* and *FUL2* have critical but redundant roles in the determination and maintenance of SM identity and that *FUL3* has a limited effect on this trait.

Transcript levels of *SHORT VEGETATIVE PHASE* (*SVP*)-like MADS-box genes *VRT2*, *BM1* and *BM10* are upregulated in the developing spikes of the *vrn1ful2*-null mutant

A partial reversion of basal spikelets to vegetative tillers, similar to the one described above for the *vrn1ful2*-null mutant, has been described in barley lines overexpressing *SVP*-MADS-box genes *BM1* or *BM10* (see Discussion). To test if the transcript levels of the *SVP*-like wheat genes were affected in the *vrn1ful2*-null mutants, we first studied their expression during normal spike development in Kronos. Transcript levels of three related paralogs *BM1*, *BM10* and *VRT2* (RefSeq v1.0 gene designations in Fig. S6) decreased three- to five-fold from the initial stages of spike development (W2, Waddington scale) to the floret primordium stage (W3.5, Fig. S6A-C).

Then, we compared the transcriptional levels of the *SVP*-like wheat genes in *vrn1ful2*-null and *vrn1*-null mutants. Plants were grown for 53 days in the same growth chamber until the developing spikes of *vrn1*-null were at the terminal spikelet stage and those from *vrn1ful2*-null had a similar number of lateral meristems (Fig. 2D and H). The transcript levels of wheat *BM1*, *BM10* and *VRT2* in the developing spikes were roughly ten-fold higher in the *vrn1ful2*-null mutant than in the *vrn1*-null and control lines ($P < 0.0001$, Fig. S6D-F). These results suggest that *VRN1* and *FUL2* are either direct or indirect transcriptional repressors of the three wheat *SVP*-like genes.

***FUL2* and *VRN1* have redundant roles on spike determinacy and regulate the number of spikelets per spike**

Normal wheat spikes are determinate, with the distal IM transitioning into a terminal spikelet after producing a relatively stable number of lateral meristems (Fig. 4A). In *vrn1ful2*-null, by contrast, the spike-like structures are indeterminate, with a distal IM that continues to produce lateral meristems while growing conditions are favorable (Fig. 4B). In the *ful2*-null background, one functional copy of *VRN1* in the heterozygous state was sufficient to generate a determinate spike (Fig. 3D, *ful2*-null/*vrn-A1*-null *vrn-B1*), and the same was true for a single functional copy of *FUL2* in a *vrn1*-null background (Fig. 3K, *vrn1*-null/*ful2-A Ful2-B*).

The individual *vrn1*-null and *ful2*-null mutants (in a homozygous state) showed a larger number of spikelets per spike than the control. This increase was 58% in the *vrn1*-null mutant ($P < 0.0001$, Fig. 4C) and 10% in the *ful2*-null mutant ($P = 0.0014$, Fig 4D). Although no significant increases in the number of spikelets per spike were detected in the individual *ful3*-null mutant ($P = 0.4096$, Fig. 4E), two independent transgenic lines overexpressing *FUL3* (*Ubi::FUL3*) showed an average reduction of 1.12 spikelet per spike relative to their non-transgenic sister lines ($P = 0.0132$ and $P < 0.0001$, Fig. S7A). This last result indicates that *FUL3* can still play a role on the timing of the transition of the IM to a terminal spikelet.

A similar reduction in the number of spikelets per spike was observed in two independent *Ubi::FUL2* transgenic lines (1.05 spikelets per spike reduction, $P < 0.03$, Fig. S7B). We then investigated the effect of this transgene in the presence of different *VRN1* and *VRN2* alleles in the same F_2 population described previously (*Ubi::FUL2* x *vrn1vrn2*-null). In the *vrn2*-null F_2 plants, the differences in spikelet number between *Ubi::FUL2* and wild type alleles were larger in *vrn1*-null than in the *Vrn1*-Het plants (interaction $P < 0.0001$, Fig. S7C). In a separate group of F_2 plants fixed for *Vrn1*-Het and segregating for *VRN2* and *FUL2*, we did not detect significant effects for *Ubi::FUL2* and the interaction was not significant (Fig. S7D). However, we observed 3.3 more spikelets per spike in *Vrn2*-wt than in *vrn2*-null plants ($P < 0.0001$, Fig. S7D). These results suggest that the strong *Vrn-A1* allele for spring growth habit can mask the effects of the *Ubi::FUL2* transgene but not that of *VRN2* on the number of spikelets per spike.

Increased transcript levels of *CEN2*, *CEN4* and *CEN5* in developing spikes of the *vrn1ful2*-null mutant

Based on the strong effect observed in the Arabidopsis *tfl1* mutant and the *Antirrhinum cen* mutant on inflorescence determinacy (see Discussion), we decided to investigate the effect of the *vrn1ful2*-null mutations on the expression levels of the *TFL1/CEN*-like wheat homologs in the developing spike. Since no previous nomenclature was available for the wheat *CEN* paralogs, we assigned them numbers to match their chromosome locations, and designated them as *CEN2*, *CEN4* and *CEN5* (RefSeq v1.0 designations can be found in the legend of Fig. S8). The transcript levels of these three genes were downregulated as the developing spike progressed from the double-ridge stage to the floret primordium stage (Waddington scale 2 to 3.5, Fig. S8A-C).

Comparison of *vrn1ful2*-null and *vrn1*-null plants grown for 53 days in the same growth chamber (Fig. 2D and H) showed that the transcript levels of *CEN2*, *CEN4* and *CEN5* were significantly higher ($P < 0.0001$) in the developing spikes of the *vrn1ful2*-null mutant than in those of the *vrn1*-null mutant or the Kronos control (all in *vrn2*-null background). These differences were larger for *CEN2* and *CEN4* than for *CEN5* (Fig. S8D-F). Taken together, these results suggested that *VRN1* and *FUL2* work as transcriptional repressors of the *TFL1/CEN*-like wheat homologs.

The *ful2*-null mutant produces a higher number of florets per spikelet and more grains per spike in the field

In addition to the higher number of spikelets per spike, the *ful2*-null mutant showed a higher number of florets per spikelet than the Kronos control, an effect that was not observed for *vrn1*-null (Fig. 2B-C) or *ful3*-null (Fig. S5A). The average increase in floret number was similar in *ful2*-null (1.3 florets) and *ful2ful3*-null (0.9 florets), suggesting that *FUL3* has a limited effect on this trait. In spite of some heterogeneity in the distribution of spikelets with extra florets among spikes, the differences between the control and the *ful2*-null mutants were significant at all spike positions (Fig. S5B).

Similar increases in the number of florets per spikelet were reported before in Kronos plants overexpressing *miRNA172* (*Ubi::miR172*, (Debernardi et al., 2017). To study the genetic interactions between *Ubi::miR172* and *ful2*-null we crossed the transgenic and mutant lines and studied their effects on floret number in the progeny using a two-way factorial ANOVA. We detected significant differences in average floret number for both *ful2*-null and *Ubi::miR172* ($P < 0.01$) and a marginally significant interaction ($P < 0.0435$) that can be visualized in the

interaction graph in Fig. S5C. The differences in average floret number between *ful2*-null and the wild type control were larger (and more variable) in the *Ubi::miR172* than in the non-transgenic background (Fig. S5C-F). Both the mutant and transgenic lines showed heterogeneity among spikes in the location of spikelets with increased numbers of florets (Fig. S5D-F).

Based on its positive effect on the number of florets per spikelet and spikelets per spike (and its small effect on heading time), we selected the *ful2*-null mutant for evaluation in a replicated field experiment. Relative to the control, the *ful2*-null mutant produced 20% more spikelets per spike (P = 0.0002) and 9% more grains per spikelet (P= 0.05), which resulted in a 31% increase in the number of grains per spike (P = 0.0002, Fig. 4F). In this experiment, part of the positive effect on grain yield was offset by a 19% reduction in average kernel weight (P = 0.0012). In spite of these opposite trends, we observed a slight net increase of 6% in total grain weight per spike (P = 0.09, Fig. 4F). This negative correlation between grain number and grain weight suggest that in this particular genotype by environment combination grain yield was more limited by the "source" (produced and transported starch) than by the "sink" (number and size of grains).

DISCUSSION

RNA *in situ* hybridization studies at the early double-ridge stage of spike development in wheat (Preston and Kellogg, 2008) and *Lolium temulentum* (Gocal et al., 2001) have shown that both *VRN1* and *FUL2* are expressed in the spike apical meristem and in spikelet primordia. Based on their shared localization it was hypothesized that these two genes might have overlapping roles in spike development. This study provides experimental evidence for this hypothesis and demonstrates that *FUL2* and *VRN1* play central but redundant roles in the determination of spikelet meristem identity and spike determinacy. It also shows that mutations in these two genes, and in the more distantly related *FUL3* paralog, affect wheat heading time and stem elongation.

Mutations in *VRN1*, *FUL2* and *FUL3* reduce stem elongation

No effects on stem elongation had been reported previously for *VRN1*, *FUL2* or *FUL3* in wheat or *AP1*, *CAL* or *FUL* mutants in Arabidopsis, so we initially paid little attention to this trait. However, differences in stem elongation in the double- and triple-null mutants were too obvious

to be ignored. The small effects of the single *vrn1*-null and *ful3*-null mutants were magnified in the *vrn1ful3*-null mutant, indicating a synergistic interaction (Fig. S3B). A similar synergistic interaction was detected when the *ful2*-null mutant (Fig. S3C) was combined with the *vrn1*-null and *ful3*-null mutations (Fig. S3D-E). These results suggest that *VRN1*, *FUL2* and *FUL3* have redundant functions in the regulation of stem elongation, and that their individual effects are magnified in the absence of the other paralogs.

Although the molecular mechanisms by which these genes affect stem elongation are currently unknown, an indirect way by which *VRN1* may contribute to this trait is through its strong effect on the regulation of *FT1*. The induction of *FT1* has been shown to result in the upregulation of gibberellic acid (GA) biosynthetic genes in developing wheat spikes (Pearce et al., 2013). GA biosynthesis and sensitivity are known to play critical roles in the determination of stem elongation in wheat (Peng et al., 1999). Therefore, the downregulation of *FT1* in the *vrn1*-null mutant (Chen and Dubcovsky, 2012) is expected to reduce GA levels, which would inhibit stem elongation.

A loss-of-function mutation in a homolog of *AP1* in rapeseed resulted in increased plant height by 7.6 cm (Shah et al., 2018). This effect is opposite to what we observed in the loss-of-function mutations in the wheat homologs, which suggests that different mechanisms are involved in the effect of this group of meristem identity genes on plant height in these two species.

Mutations in *VRN1*, *FUL2* and *FUL3* delay flowering initiation in wheat

VRN1 is one of the main genes controlling natural variation in wheat flowering time (Fu et al., 2005; Kippes et al., 2016; Yan et al., 2003; Zhang et al., 2008), so it was not surprising that *vrn1*-null delayed heading time more than *ful2*-null or *ful3*-null. Although the strong *Vrn-A1* allele for spring growth habit masked the smaller effects of *FUL2* and *FUL3* (Fig. 1A-C), in the absence of *VRN1* the *FUL2* and *FUL3* mutants showed delayed flowering initiation(Fig. 1D), indicating that *FUL2* and *FUL3* have retained some residual functionality in the acceleration of wheat flowering time. This was further confirmed by the accelerated flowering of the *Ubi::FUL2* and *Ubi::FUL3* transgenic plants (Fig. 1 E-F). Similar results have been reported in *Brachypodium distachyon,* in which overexpression of *VRN1* (Ream et al., 2014)*, FUL2* or *FUL3* (Li et al., 2016) accelerates flowering, and downregulation of *VRN1* delays flowering relative to non-transgenic controls

(Woods et al., 2016). These results suggest a conserved role of these genes in the regulation of flowering time in temperate grasses.

Previous studies have shown a significant interaction between wheat *VRN1* and *VRN2* in the regulation of heading time (Tranquilli and Dubcovsky, 2000). This study shows that similar interactions exist between *FUL2* and *VRN2* (Fig. 1G-H). A tetraploid wheat population segregating for *VRN1*, *FUL2* and *VRN2* revealed highly significant two-way and three-way interactions among these genes, indicating that the effect of each of these genes on heading time is dependent on the particular combination of alleles present for the other two. Previous studies have shown that part of the ability of *VRN1* to accelerate flowering depends on its ability to repress *VRN2* (Chen and Dubcovsky, 2012). The larger effect on heading time of the *Ubi::FUL2* transgene in the presence of the functional *Vrn2* than in the *vrn2*-null background (Fig. 1G-H) suggests that *FUL2* repression of *VRN2* can also contribute to its ability to accelerate heading time.

***VRN1* and *FUL2* play critical and redundant roles in spikelet and floral development**

The most significant discovery from this study was the central and redundant roles of *VRN1* and *FUL2* in the specification of the spikelet meristem identity. Even though the VM to IM transition was not impaired in the *vrn1ful2*-null mutant, these plants were unable to form normal spikelets. The *vrn1ful2*-null and *vrn1ful2ful3*-null mutants showed an elongated stem terminating in a spike-like structure (Fig. 2A) with lateral meristems arranged in a distichous phyllotaxis, similar to normal spikes (Fig. 2H, I, K and Fig. 4A-B). However, the fate of the lateral meristems was drastically different in the wild type and mutant genotypes. In the wild type, the lateral meristems acquired SM identity and formed normal spikelets with fertile flowers, whereas in the *vrn1ful2*-null and *vrn1ful2ful3*-null mutants the lateral meristems reverted to VMs that formed leaves. Interestingly, after forming a few leaves these VMs transitioned again into IMs with lateral VMs, generating a recurrent developmental cycle that ended with the death of the plant.

No normal spikelets were observed in the double *vrn1ful2*-null mutant, but some of the tillers in the basal region of the spike-like structure showed leafy bracts subtending abnormal floral organs in the position of the first floret. This result indicates that *VRN1* and *FUL2* are not absolutely essential for the production of floral organs. This was also observed in the Arabidopsis *ap1calful* mutants, which usually failed to produce flowers but were able to produce

some abnormal floral organs under high temperatures (Ferrándiz et al., 2000). In Arabidopsis, AP1 orchestrates a network of intermediate transcription factors that promote FM identity genes and repress VM or IM identity genes (Kaufmann et al., 2010). The escape of these intermediate transcription factors from AP1 control in old plants or under particular stress conditions occasionally resulted in the formation of floral organs in the Arabidopsis *ap1calful* mutant.

Among the transcription factors directly repressed by AP1, the MADS-box *SVP* and *AGAMOUS-LIKE 24* (*AGL24*) play important roles in the formation of floral meristems (Kaufmann et al., 2010; Liu et al., 2007). In the absence of AP1, ectopic expression of *SVP* and *AGL24* transform floral meristems into shoot meristems (Liu et al., 2007). The three related *SVP*-like genes in wheat and barley lineages (*VRT2*, *BM1* and *BM10*) originated from duplications independent of the one that originated *SVP* and *AGL24* in Arabidopsis and, therefore, have independent subfunctionalization stories (Trevaskis et al., 2007). Overexpression of *BM1* and *BM10* in barley plants grown under short days resulted in the formation of vegetative tillers in the base of the spike (Trevaskis et al., 2007), which were similar to the tillers formed in the spike-like structures described in the wheat *vrn1ful2*-null spikes in this study. Based on these observations, we hypothesize that the 10-fold upregulation of *VRT2*, *BM1* and *BM10* transcripts detected in the *vrn1ful2*-null mutants (Fig. S6) may have contributed to the reversion of the lateral SMs into VMs.

FUL2 mutants increase the number of florets per spikelet

In wheat, the spikelet meristem is indeterminate and can initiate a variable number of floret primordia. Most of these primordia are aborted during spikelet development, a process that is affected by genetic differences (Guo et al., 2016; Sakuma et al., 2018), photoperiod (Gonzalez et al., 2005), plant height (Miralles et al., 1998), and available resources (Ferrante et al., 2013). An increase in the number of florets per spikelet was detected in *ful2*-null but not in *vrn1*-null and *ful3*-null, which suggests that among these three paralogs only *FUL2* contributes to maintaining a limited number of florets per spikelet (Fig. S5B). Since a higher number of florets per spikelet can contribute to a higher grain yield potential, it would be interesting to explore the natural variation in *FUL2* and its effect on this trait.

Overexpression of wheat *miR172* or loss of function mutations in its *AP2-5* target also result in higher number of florets per spikelet (Debernardi et al., 2017). The synergistic interaction

detected in this study between miR172 and *ful2*-null for this trait (Fig. S5C) suggests that *miR172/AP2-5* and *FUL2* may control floret number through a common pathway. However, the actual mechanism by which *FUL2* contributes to maintaining a low number of florets per spikelets is currently unknown. Since loss-of-function mutations in *FT2* also affect the number of florets per spike (Shaw et al., 2018), we have initiated crosses between *ft2*-null and *ful2*-null to investigate their genetic interactions.

***VRN1* and *FUL2* have essential and redundant roles in wheat spike determinacy**

The determinate growth of the wheat spike requires the transition of the distal IM into a SM and the formation of a terminal spikelet. The *vrn1ful2*-null mutant was unable to form spikelets, so it was not surprising that it was unable to form a terminal spikelet (Fig. 2H and 4B). However, the fate of the terminal and lateral meristems in *vrn1ful2*-null was different, with the lateral meristems reverting to VMs and the terminal IM remaining indeterminate. The IM seems to be very sensitive to the activity of *FUL2* or *VRN1*, since a single functional copy of either of these genes in a heterozygous state was sufficient to restore spike determinacy (Fig 3D and K).

Loss-of-function mutations in *TERMINAL FLOWER 1* (*TFL1*) in Arabidopsis or in the *CENTRORADIALIS* (*CEN*) homolog in *Antirrhinum* result in the formation of a terminal flower and the transformation of indeterminate into determinate inflorescences (Bradley et al., 1997; Ratcliffe et al., 1999). In Arabidopsis, *TFL1* is a direct target of AP1 (Kaufmann et al., 2010), and the *ap1cal* and *ap1calful* mutants show *TFL1* upregulation and ectopic expression in young lateral meristems preventing the formation of flowers (Ferrándiz et al., 2000; Ratcliffe et al., 1999). The rice *CEN* homologs (*RCN1*-*RCN4*) also repress floral fate and affect inflorescence architecture (Kaneko-Suzuki et al., 2018; Nakagawa et al., 2002), which suggests conserved functions across distantly divergent plant lineages. Based on this conservation, it is tempting to speculate that the upregulation of the wheat *CEN2*, *CEN4* and *CEN5* homologs in the developing spike of the *vrn1ful2*-null mutant might have contributed to its indeterminate growth.

The *vrn1*-null and *ful2*-null mutants have a higher number of spikelets per spike

In wheat, the timing of the transition between the IM and the terminal spikelet determines the number of spikelets per spike. Since *VRN1* and *FUL2* play a central role in this transition, we hypothesized that changes in their dosage could affect the number of spikelets per spike. This

418 hypothesis was confirmed in the single *vrn1*-null and *ful2*-null mutants, which showed increases
419 of nine and two spikelets per spike respectively (Fig. 4C-D). The stronger effect of *vrn1*-null
420 relative to *ful2*-null on spikelet number is likely associated with *VRN1*'s stronger effect on
421 heading time (Fig. 1A-C), which results in a longer period of spike development, thereby
422 providing more time for the formation of additional spikelets. A stop codon mutation in a
423 homolog of AP1 in rapeseed altered plant architecture and increased the number of seeds per
424 plant (Shah et al., 2018), suggesting that mutations in this group of meristem identity genes may
425 be useful to modulate seed number in other species.

426 In the field study, the *ful2*-null plants showed a 30.8% increase in the average number of grains
427 per spike compared with the control sister lines. This large increase was likely a result of the
428 simultaneous increase in the number of spikelets per spike and florets per spikelet in this mutant.
429 Although in this experiment the positive increase in grain number was partially offset by a
430 decrease in average grain weight, the total grain weight per spike was still slightly higher (6.3%)
431 in the *ful2*-null mutant. It would be interesting to test if the introgression of this mutation in
432 genotypes which higher biomass (increased "source") can reduce the negative correlation
433 between grain number and grain weight. In addition, optimum agronomic conditions will be
434 required to translate the *ful2*-null increase in grain number into larger increases in total grain
435 yield.

436 The results presented here indicate that *VRN1* and *FUL2* play key and redundant roles in the
437 development of the spikelet, the reproductive structure that defines the grass family. Moreover,
438 our results indicate that these two genes are required for the determinate growth of the wheat
439 spike, and that loss-of-function of either gene affect the number of spikelets per spike, which is
440 an important component of grain yield. In summary, our results suggest that a better
441 understanding of the processes that control the development of grass flowers and inflorescences
442 may contribute to improving the productivity of a group of cereal crop species that is critical for
443 the global food supply.

444 **ACKNOWLEDGEMENTS**

445 This project was supported by the Howard Hughes Medical Institute, NRI Competitive Grant
446 2016-67013-24617 from the USDA National Institute of Food and Agriculture (NIFA) and the
447 International Wheat Partnership Initiative (IWYP). We thank Dr. Alejandra Alvarez and Dr. Josh

Hegarty for their help with field experiments and Dr. Daniel Wood and Dr. Juan Debernardi for their valuable comments and suggestions.

COMPETING FINANCIAL INTERESTS STATEMENT

The authors declare no conflict of interest.

AUTHOR CONTRIBUTIONS

CL and JD designed research; JD provided overall supervision to the project; HL, CL, AC, ML and JJ performed research; CL, HL and JD analyzed data; JD provided statistical analyses; CL wrote first draft and JD the final version. All authors reviewed the paper.

MATERIALS AND METHODS

Selected mutations and mutant combinations

An ethyl methane sulphonate (EMS) mutagenized population of the tetraploid wheat variety Kronos was screened for mutations initially using *Cel*I assays (Uauy et al., 2009) and later using BLAST searches in the database of sequenced mutations for the same population (Krasileva et al., 2017). We identified loss-of-function mutations in the A and B genome homeologs of *FUL2* and *FUL3*, which were confirmed using genome specific primers described in Table S1. Single genome mutants were backcrossed two to three times to Kronos *vrn2*-null to reduce background mutations. A Kronos *vrn2*-null line with no functional copies of the *VRN2* flowering repressor (Distelfeld et al., 2009) was used as recurrent parent to avoid the extremely late flowering of mutant combinations including the *vrn1*-null. All mutants described in this study are in a *vrn2*-null background unless indicated otherwise.

For *FUL-A2*, we selected line T4-837 (henceforth *ful-A2*), which has a mutation in the splice donor site of the fifth intron. RT-PCR and sequencing analysis of the *ful-A2* transcripts revealed two incorrect splicing forms. The most abundant form skipped the fifth exon, which resulted in a deletion of 14 amino acids in the middle of the K-box (Δ144-157). In the other alternative splicing form, the retention and translation of the fifth intron generated a premature stop codon that disrupted the K-box and removed the entire C-terminus (Fig. S2A). For *FUL-B2*, we selected line T4-2911 that carries a C to T change at nucleotide 484 (henceforth *ful-B2*). The *ful-*

478 *B2* mutation generates a premature stop codon at position 162 (Q162*) that removed the last 13
479 amino acids of the K-box and the entire C-terminus (Fig. S2A).

480 For *FUL-A3*, we selected line T4-2375 that carries a G to A mutation in the splice acceptor site
481 of the third intron. Sequencing of *ful-A3* transcripts revealed that this mutation generated a new
482 splice acceptor site that shifted the reading frame by one nucleotide. The alternative translation
483 generated a premature stop codon that truncated 72% of the K-box and the entire C-terminus
484 (Fig. S2B). For *FUL-B3*, we selected line T4-2139 that carries a C to T mutation at nucleotide
485 position 394 that generates a premature stop codon at amino acid position 132 (Q132*). This
486 premature stop removed half of the K-box and the complete C-terminus (Fig. S2B). Given the
487 critical roles of the K-domain in protein-protein interactions, and the C-terminal domain in
488 transcriptional activation, these selected mutations are expected to impair the normal function of
489 the FUL2 and FUL3 proteins.

490 The A and B-genome mutants for each gene were intercrossed to generate double mutants, which
491 for simplicity, are referred to hereafter as null mutants. The *ful2*-null and *ful3*-null were
492 intercrossed with a *vrn1vrn2*-null mutant (*vrn-A1*-null T4-2268 / *vrn-B1* T4-2619 / *vrn2*-null)
493 (Chen and Dubcovsky, 2012) to generate *vrn1ful2*-null and *vrn1ful3*-null, which were finally
494 intercrossed to generate *vrn1ful2ful3*-null (all in a *vrn2*-null background). The *vrn1ful2*-null and
495 *vrn1ful2ful3*-null mutants were sterile, so they were maintained and crossed by keeping the *ful-*
496 *B2* mutation in heterozygous state.

497 Transgenic Kronos plants overexpressing *FUL2* and *FUL3* coding regions were generated at the
498 UC Davis Transformation facility using *Agrobacterium*-mediated transformation. The coding
499 regions of these two genes were cloned from Kronos into the binary vector pLC41 (Japan
500 Tobacco, Tokyo, Japan) downstream of the maize *UBIQUITIN* promoter. A C-terminal 3xHA
501 tag was added to FUL2 and a C-terminal 4xMYC tag was added to FUL3. Mutant and transgenic
502 wheat plants were grown in PGR15 CONVIRON chambers under LD (16h light/8h dark, light
503 intensity ~330 μM m^{-2} s^{-1}) at 22 ºC during the day and 18 ºC during the night.

504 To study the effect of *Ubi::FUL2* in different genetic backgrounds we crossed the Kronos
505 *Ubi::FUL2* with Kronos-*vrn1vrn2*-null and analyzed the effect of the three genes in the F_2
506 progeny under greenhouse conditions. A field experiment comparing *ful2*-null and its control
507 line was performed at the University of California, Davis field station during the 2017-2018

508 growing season (sowed on 12/1/2017 and harvested on 06/25/2018). One meter rows (30 grains
509 per row) were used as experimental units and the experiment was organized in a randomized
510 complete block design with eight blocks. During the growing season plants received 200 units of
511 N as ammonium sulfate, three irrigations, one application of broad-leaf herbicides (2, 4D +
512 Buctril) and alternating applications of fungicides Quadris and Tilt every 2 weeks.

513 **Effect of the splice site mutations in *ful-A2* and *ful-B3* mutants**

514 To determine the effect of the splice site mutations in *ful-A2* and *ful-B3*, we extracted total RNA
515 from leaf samples using the Spectrum™ Plant Total RNA kit. cDNA was synthesized from 2 µg
516 of RNA using the High Capacity Reverse Transcription Kit according to the manufacturer's
517 instructions and used as RT-PCR template. For *ful-A2*, we used primers *FUL2-837-F* (5'-
518 CCATACAAAAATGTCACAAGC-3') and *FUL2-837-R* (5'-TTCTGC CTCTCCACCAGTT-3')
519 for RT-PCR. These primers, which are not genome specific, amplified three fragments of 303 bp,
520 220 bp and 178 bp. We gel-purified these fragments, cloned them into pGEM-T vector
521 (Promega), and sequenced them. The 220 bp fragment was from the wild type *FUL-B2* allele,
522 whereas the other two fragments corresponded to two alternative splicing forms of *ful-A2* that
523 either retained the fifth intron (303 bp) or skipped the fifth exon (178 bp).

524 For the *ful-B3* mutant, we performed RT-PCR using primers FUL3-2375-F (5'-
525 ATGGATGTGATTCTTGAAC-3') and FUL3-2375-R (5'-
526 TGTCCTGCAGAAGCACCTCGTAGAGA-3'). Sequencing analysis of the PCR products
527 showed that the G to A mutation generated a new splice acceptor site with an adjacent G that
528 shifted the reading frame by one nucleotide after 333 bp, and generated a premature stop codon.

529 **Scanning Electron-Microscopy (SEM)**

530 Apices from different developmental stages were dissected and fixed for a minimum of 24 h in
531 FAA (50% ethanol, 5% (v/v) acetic acid, 3.7% (v/v) formaldehyde), and then dehydrated
532 through a graded ethanol series to absolute ethanol. Samples were critical-point dried in liquid
533 CO2 (tousimis ® 931 Series critical point drier), mounted on aluminum stubs, sputter-coated
534 with gold (Bio-Rad SEM Coating System Model E5100), and examined with a Philips XL30
535 scanning electron-microscope operating at 5KV. Images were recorded at slow scan 3 for high
536 definition and saved as TIFF files.

RNA extraction and Real-time qPCR analysis

RNAs from apices were extracted using the Trizol reagent (ThermoFisher Scientific, Cat. No.15596026). One µg of RNA was used for cDNA synthesis following the instructions of the "High-Capacity cDNA Reverse Transcription Kit" (ThermoFisher Scientific, Cat. No. 4368814). The cDNA was then diluted 20 times and 5 µl of the dilution was mixed with 2×VeriQuest Fast SYBR Green qPCR Master Mix (Affymetrix, Cat. No. 75690) and with primers for the real-time qPCR analysis. Primer sequences are listed in Table S2. *INNITIATION FACTOR 4A* (*IF4A*) was used as an endogenous control. Transcript levels for all genes are expressed as linearized fold-*IF4A* levels calculated by the formula $2^{(IF4A\ C_T - TARGET\ C_T)}$ ± standard error (SE) of the mean. The resulting number indicates the ratio between the initial number of molecules of the target gene and the number of *IF4A* molecules.

549 **REFERENCES**

550 **Bradley, D., Ratcliffe, O., Vincent, C., Carpenter, R. and Coen, E.** (1997). Inflorescence
551 commitment and architecture in Arabidopsis. *Science* **275**, 80-83.

552 **Chen, A. and Dubcovsky, J.** (2012). Wheat TILLING mutants show that the vernalization gene
553 *VRN1* down-regulates the flowering repressor *VRN2* in leaves but is not essential for flowering.
554 *PLoS Genetics* **8**, e1003134.

555 **Ciaffi, M., Paolacci, A. R., Tanzarella, O. A. and Porceddu, E.** (2011). Molecular aspects of
556 flower development in grasses. *Sexual Plant Reproduction* **24**, 247-282.

557 **Debernardi, J. M., Lin, H., Chuck, G., Faris, J. D. and Dubcovsky, J.** (2017). microRNA172
558 plays a crucial role in wheat spike morphogenesis and grain threshability. *Development* **144**,
559 1966-1975.

560 **Distelfeld, A., Tranquilli, G., Li, C., Yan, L. and Dubcovsky, J.** (2009). Genetic and
561 molecular characterization of the *VRN2* loci in tetraploid wheat. *Plant Physiology* **149**, 245-257.

562 **Ferrándiz, C., Gu, Q., Martienssen, R. and Yanofsky, M. F.** (2000). Redundant regulation of
563 meristem identity and plant architecture by *FRUITFULL*, *APETALA1* and *CAULIFLOWER*.
564 *Development* **127**, 725-734.

565 **Ferrante, A., Savin, R. and Slafer, G. A.** (2013). Floret development and grain setting
566 differences between modern durum wheats under contrasting nitrogen availability. *Journal of*
567 *Experimental Botany* **64**, 169-184.

568 **Fu, D., Szűcs, P., Yan, L., Helguera, M., Skinner, J., Hayes, P. and Dubcovsky, J.** (2005).
569 Large deletions within the first intron in *VRN-1* are associated with spring growth habit in barley
570 and wheat. *Molecular Genetics and Genomics* **273**, 54-65.

571 **Gocal, G. F. W., King, R. W., Blundell, C. A., Schwartz, O. M., Andersen, C. H. and**
572 **Weigel, D.** (2001). Evolution of floral meristem identity genes. Analysis of *Lolium temulentum*
573 genes related to *APETALA1* and *LEAFY* of Arabidopsis. *Plant Physiology* **125**, 1788-1801.

574 **Gonzalez, F. G., Slafer, G. A. and Miralles, D. J.** (2005). Floret development and survival in
575 wheat plants exposed to contrasting photoperiod and radiation environments during stem
576 elongation. *Functional Plant Biology* **32**, 189-197.

577 **Guo, Z. F., Slafer, G. A. and Schnurbusch, T.** (2016). Genotypic variation in spike fertility
578 traits and ovary size as determinants of floret and grain survival rate in wheat. *Journal of*
579 *Experimental Botany* **67**, 4221-4230.

580 **Honma, T. and Goto, K.** (2001). Complexes of MADS-box proteins are sufficient to convert
581 leaves into floral organs. *Nature* **409**, 525-9.

582 **Kaneko-Suzuki, M., Kurihara-Ishikawa, R., Okushita-Terakawa, C., Kojima, C., Nagano-**
583 **Fujiwara, M., Ohki, I., Tsuji, H., Shimamoto, K. and Taoka, K. I.** (2018). TFL1-Like
584 proteins in rice antagonize rice FT-like protein in inflorescence development by competition for
585 complex formation with 14-3-3 and FD. *Plant and Cell Physiology* **59**, 458-468.

586 **Kaufmann, K., Wellmer, F., Muino, J. M., Ferrier, T., Wuest, S. E., Kumar, V., Serrano-**
587 **Mislata, A., Madueno, F., Krajewski, P., Meyerowitz, E. M. et al.** (2010). Orchestration of
588 floral initiation by APETALA1. *Science* **328**, 85-89.

589 **Kellogg, E. A.** (2001). Evolutionary history of the grasses. *Plant Physiology* **125**, 198-1205.

590 **Kellogg, E. A., Camara, P. E. A. S., Rudall, P. J., Ladd, P., Malcomber, S. T., Whipple, C.**
591 **J. and Doust, A. N.** (2013). Early inflorescence development in the grasses (Poaceae). *Frontiers*
592 *in Plant Science* **4**.

593 **Kippes, N., Chen, A., Zhang, X., Lukaszewski, A. J. and Dubcovsky, J.** (2016). Development
594 and characterization of a spring hexaploid wheat line with no functional *VRN2* genes.
595 *Theoretical and Applied Genetics* **129**, 1417–1428.

596 **Krasileva, K. V., Vasquez-Gross, H., Howell, T., Bailey, P., Paraiso, F., Clissold, L.,**
597 **Simmonds, J., Ramirez-Gonzalez, R. H., Wang, X., Borrill, P. et al.** (2017). Uncovering
598 hidden variation in polyploid wheat. *Proceedings of the National Academy of Sciences of the*
599 *United States of America* **114**, E913–E921

600 **Li, Q., Wang, Y., Wang, F. X., Guo, Y. Y., Duan, X. Q., Sun, J. H. and An, H. L.** (2016).
601 Functional conservation and diversification of *APETALA1/FRUITFULL* genes in *Brachypodium*
602 *distachyon*. *Physiologia Plantarum* **157**, 507-518.

603 **Liu, C., Zhou, J., Bracha-Drori, K., Yalovsky, S., Ito, T. and Yu, H.** (2007). Specification of
604 Arabidopsis floral meristem identity by repression of flowering time genes. *Development* **134**,
605 1901-1910.

606 **Malcomber, S. T., Preston, J. C., Reinheimer, R., Kossuth, J. and Kellogg, E. A.** (2006).
607 Developmental gene evolution and the origin of grass inflorescence diversity. *Advances in*
608 *Botanical Research* **44**, 425-481.

609 **Miralles, D. J., Katz, S. D., Colloca, A. and Slafer, G. A.** (1998). Floret development in near
610 isogenic wheat lines differing in plant height. *Field Crops Research* **59**, 21-30.

611 **Nakagawa, M., Shimamoto, K. and Kyozuka, J.** (2002). Overexpression of *RCN1* and *RCN2*,
612 rice *TERMINAL FLOWER 1/CENTRORADIALIS* homologs, confers delay of phase transition
613 and altered panicle morphology in rice. *Plant Journal* **29**, 743-750.

614 **Pearce, S., Vanzetti, L. S. and Dubcovsky, J.** (2013). Exogenous gibberellins induce wheat
615 spike development under short days only in the presence of *VERNALIZATION 1*. *Plant*
616 *Physiology* **163**, 1433–1445.

617 **Peng, J. R., Richards, D. E., Hartley, N. M., Murphy, G. P., Devos, K. M., Flintham, J. E.,**
618 **Beales, J., Fish, L. J., Worland, A. J., Pelica, F. et al.** (1999). 'Green revolution' genes encode
619 mutant gibberellin response modulators. *Nature* **400**, 256-261.

620 **Preston, J. C., Christensen, A., Malcomber, S. T. and Kellogg, E. A.** (2009). MADS-box
621 gene expression and implications for developmental origins of the grass spikelet. *American*
622 *Journal of Botany* **96**, 1419-1429.

623 **Preston, J. C. and Kellogg, E. A.** (2006). Reconstructing the evolutionary history of paralogous
624 *APETALA1/FRUITFULL*-like genes in grasses (Poaceae). *Genetics* **174**, 421-437.

625 **Preston, J. C. and Kellogg, E. A.** (2008). Discrete developmental roles for temperate cereal
626 grass *VRN1*/*FUL*-like genes in flowering competency and the transition to flowering. *Plant*
627 *Physiology* **146**, 265-276.

628 **Ratcliffe, O. J., Bradley, D. J. and Coen, E. S.** (1999). Separation of shoot and floral identity in
629 Arabidopsis. *Development* **126**, 1109-1120.

630 **Ream, T. S., Woods, D. P., Schwartz, C. J., Sanabria, C. P., Mahoy, J. A., Walters, E. M.,**
631 **Kaeppler, H. F. and Amasino, R. M.** (2014). Interaction of photoperiod and vernalization
632 determines flowering time of *Brachypodium distachyon*. *Plant Physiology* **164**, 694-709.

633 **Sakuma, S., Golan, G., Guo, Z., Ogawa, T., Tagiri, A., Sugimoto, K., Bernhardt, N.,**
634 **Brassac, J., Mascher, M., Hensel, G. et al.** (2018). Unleashing floret fertility by a mutated

635 homeobox gene improved grain yield during wheat evolution under domestication. *bioRxiv*,
636 doi.org/10.1101/434985.

637 **Shah, S., Karunarathna, N. L., Jung, C. and Emrani, N.** (2018). An *APETALA1* ortholog
638 affects plant architecture and seed yield component in oilseed rape (*Brassica napus* L.). *BMC*
639 *Plant Biol* **18**, 380.

640 **Shaw, L. M., Lyu, B., Turner, R., Li, C., Chen, F., Han, X., Fu, D. and Dubcovsky, J.**
641 (2018). *FLOWERING LOCUS T2* (*FT2*) regulates spike development and fertility in temperate
642 cereals. *J Exp Bot*.

643 **Theissen, G., Melzer, R. and Rumpler, F.** (2016). MADS-domain transcription factors and the
644 floral quartet model of flower development: linking plant development and evolution.
645 *Development* **143**, 3259-3271.

646 **Tranquilli, G. and Dubcovsky, J.** (2000). Epistatic interactions between vernalization genes
647 *Vrn-A^{m}1* and *Vrn-A^{m}2* in diploid wheat. *Journal of Heredity* **91**, 304-306.

648 **Trevaskis, B., Tadege, M., Hemming, M. N., Peacock, W. J., Dennis, E. S. and Sheldon, C.**
649 (2007). *Short Vegetative Phase-like* MADS-box genes inhibit floral meristem identity in barley.
650 *Plant Physiology* **143**, 225-235.

651 **Uauy, C., Paraiso, F., Colasuonno, P., Tran, R. K., Tsai, H., Berardi, S., Comai, L. and**
652 **Dubcovsky, J.** (2009). A modified TILLING approach to detect induced mutations in tetraploid
653 and hexaploid wheat. *BMC Plant Biology* **9**, 115-128.

654 **Woods, D. P., McKeown, M. A., Dong, Y. X., Preston, J. C. and Amasino, R. M.** (2016).
655 Evolution of *VRN2/Ghd7*-like genes in vernalization-mediated repression of grass flowering.
656 *Plant Physiology* **170**, 2124-2135.

657 **Yan, L., Loukoianov, A., Tranquilli, G., Helguera, M., Fahima, T. and Dubcovsky, J.**
658 (2003). Positional cloning of wheat vernalization gene *VRN1*. *Proceedings of the National*
659 *Academy of Sciences of the United States of America* **100**, 6263-6268.

660 **Zhang, X. K., Xia, X. C., Xiao, Y. G., Dubcovsky, J. and He, Z. H.** (2008). Allelic variation at
661 the vernalization genes *Vrn-A1*, *Vrn-B1*, *Vrn-D1* and *Vrn-B3* in Chinese common wheat cultivars
662 and their association with growth habit. *Crop Science* **48**, 458-470.

663
664

FIGURE LEGENDS

Fig. 1. Effect of *FUL2* and *FUL3* on heading time under long day photoperiod. (A-F) Kronos *vrn2*-null background. (A) *vrn1*-null (n= 6) versus control (n= 6). (B) *ful2*-null (n= 8) *vs.* control (n= 11) in a *Vrn1* background. (C) *ful3*-null (n= 8) and *ful2ful3*-null (n= 15) *vs.* control (n= 10) in a *Vrn1* background. (D) Shoot apical meristem length. The red dotted line indicates the transition of the SAM to the reproductive stage (n= 6 per time point). (E-F) Heading time of Kronos T_1 transgenic plants from two independent events segregating for (E) *FUL2* (*Ubi::FUL2*, n= 4-23) and (F) *FUL3* (*Ubi::FUL3*, n= 9-31). (G-H) Two way interactions for F_2 plants segregating for *VRN1, VRN2* and *FUL2*. (G) *VRN2 x FUL2* in a *Vrn1* heterozygous background. (H) *VRN2 x FUL2* in a *vrn1*-null background. *P* values correspond to a 2 x 2 factorial ANOVA (3-way ANOVA in Table S3). Error bars are SEM. *** = $P < 0.0001$, NS = $P > 0.05$.

Fig. 2. Phenotypical characterization of the *vrn1ful2* and *vrn1ful2ful3* mutants. (A) Stems and heads of *vrn1*-null, *vrn1ful2*-null and *vrn1ful2ful3*-null mutants (leaves were removed before photography). (B-E) Phenotypes of *vrn1*-null (B) spike, (C) spikelet, and (D) dissected spike at terminal spikelet stage. (E) Scanning Electro-Microscopy (SEM) of developing spike. (F-I) *vrn1ful2*-null mutant. (F) Spike-like structure with leafy shoots replacing spikelets. (G) Detached "spikelet (shoot)" (H) Dissection of the spike-like structure showing lateral vegetative meristems and indeterminate growth (I) SEM detail of the spike-like meristem. (J-K) *vrn1ful2ful3*-null mutant. (J) Spike-like structure. (K) SEM detail of the spike-like meristems. All these mutants are in a Kronos *vrn2*-null background.

Fig. 3. **Phenotypical characterization of heterozygous mutants containing one copy of *VRN1* or *FUL2***. (A-C) *ful2*-null/*Vrn-A1* *vrn-B1*-null. (A) "Head" at early stage. (B) Detached spikelet. (C) Dissection of an individual spikelet showing floral organs including lodicules, ovaries and stamens. (D-G) *ful2*-null/*vrn-A1*-null *vrn-B1*. (D) Terminal spikelet (TS) confirming spike meristem determinacy. (E) Head at later stage. (F) Detached "spikelet" showing indeterminate growth. (G) Spikelet dissection showing rachilla elongation. (H-K) *vrn1*-null/*ful2-A* *Ful2-B* (produces viable grain). (H) Representative spikes showing formation of lateral branches in the basal region of the spike and extra florets in the terminal spikelet. (I) Detached lateral branch. (J) Dissection of the lateral branch. (K) Terminal spikelet (TS) confirming spike

meristem determinacy. Sp= spikelets, Glu= glumes, Pa= palea, Le= lemma, Ra= rachilla. All these mutants are in a Kronos *vrn2*-null background.

Fig. 4. *VRN1* and *FUL2* play redundant roles in the control of spike determinacy and affect spikelet number. (A) Scanning Electro-Microscopy of a normal wheat spike with a terminal spikelet in the *vrn1*-null control. (B) *vrn1ful2*-null mutant spike with indeterminate apical meristem. (C-E) Number of spikelets per spike in a growth chamber experiment (n=6). (C) *vrn1*-null (58% increase), (D) *ful2*-null (10% increase) and (E) *ful3*-null (no significant increase). Bars represent mean ± SEM and asterisks indicate statistically significant difference to the control line (** = $P < 0.01$, *** = $P < 0.001$, NS = $P > 0.05$). (F) ANOVAs for spike traits in *ful2*-null and sister control lines in the field (randomized complete block design with 8 blocks).

SUPPLEMENTARY FIGURES

Fig. S1. Phylogeny of duplicated Arabidopsis AP1/CAL/FUL and grasses VRN1/FUL2/FUL3 clades.

Fig. S2. Selected *ful2* and *ful3* mutations and their effect on the encoded proteins.

Fig. S3. Effect of *vrn1*-null, *ful2*-null and *ful3*-null mutations on stem length.

Fig. S4. Dissection of basal tillers from the *vrn1ful2*-null spike-like structure.

Fig. S5. Effect of *ful2*-null and *ful3*-null on the number of florets per spikelet.

Fig. S6. Transcript levels of wheat *SVP*-like MADS-box genes *VRT2*, *BM1* and *BM10*.

Fig. S7. Effect of the overexpression of *FUL2* and *FUL3* on the number of spikelets per spike.

Fig. S8. Transcript levels of wheat *TFL1/CEN*-like genes *CEN2*, *CEN4* and *CEN5*.

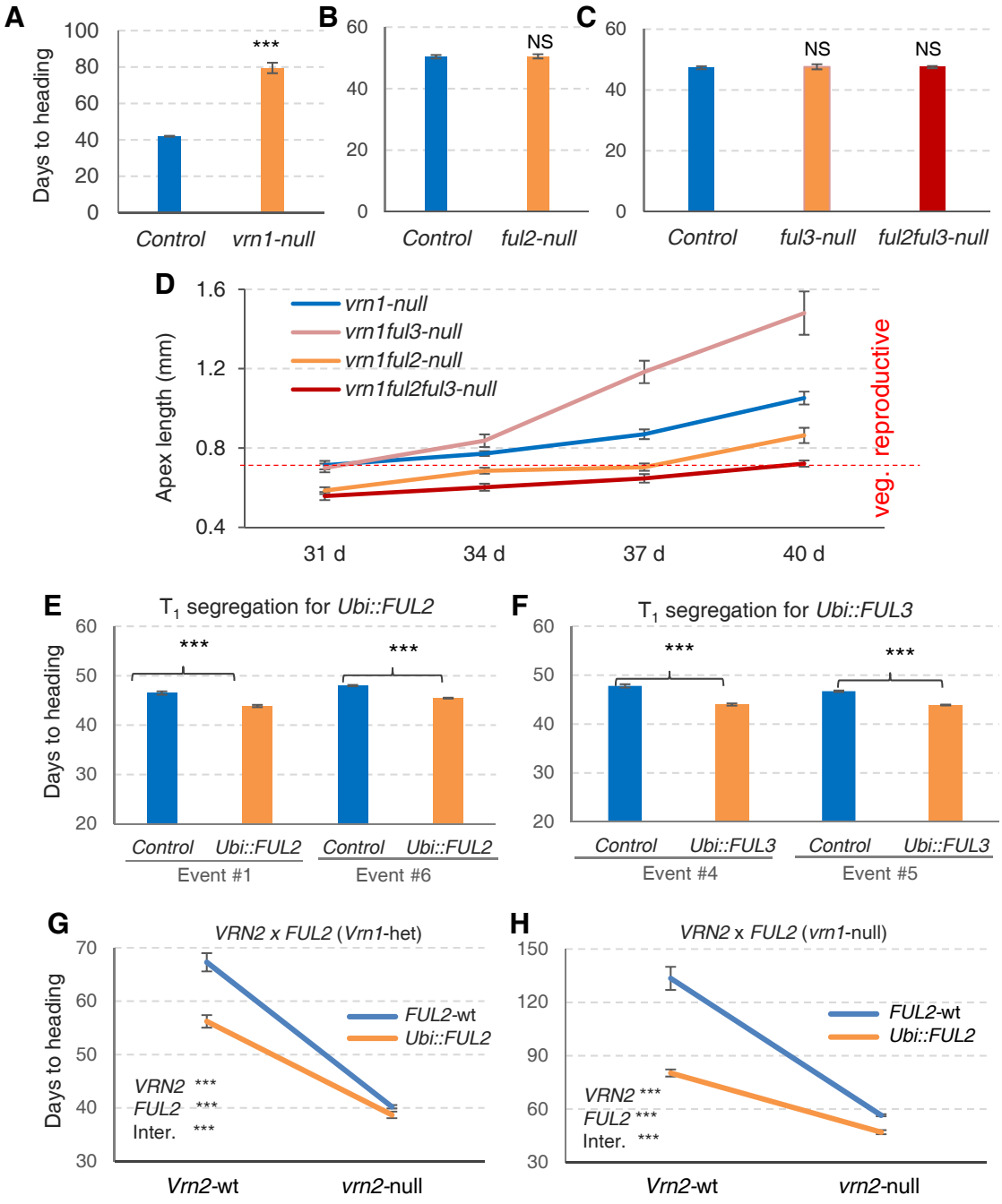

Fig. 1

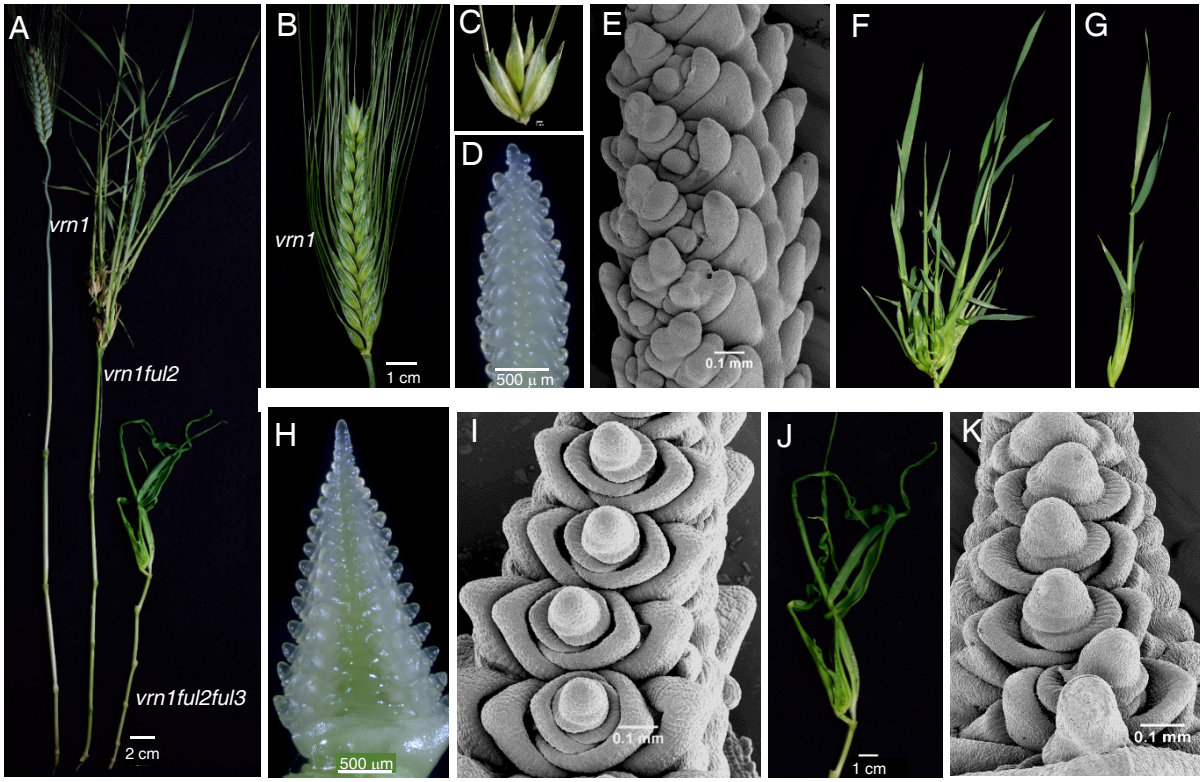

Fig. 2.

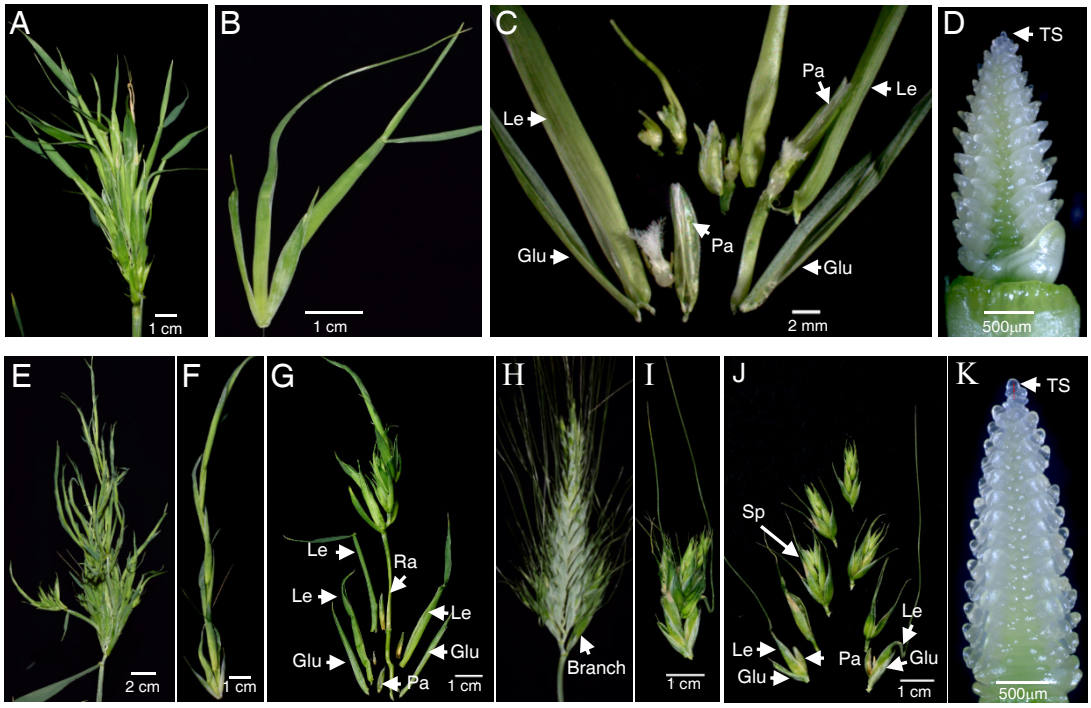

Fig. 3

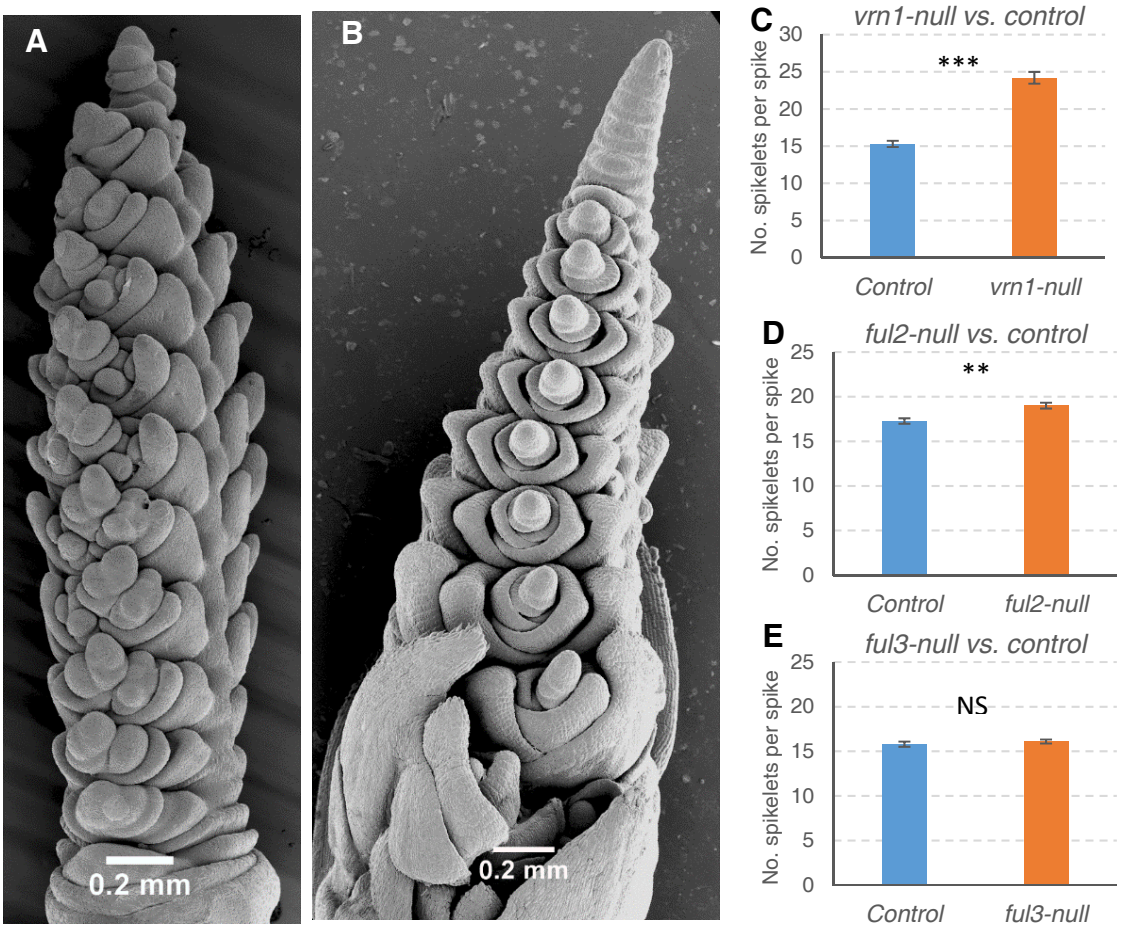

F

Field exp.	No. Spikelets /Spike	Grain No. /spike	Grain No. /spikelet	Avg. grain weight (mg)	Grain weight /spike (g)
Control	15.7	41.9	2.67	57.7	2.41
ful2-null	18.9	54.8	2.91	47.0	2.57
% diff. of control	20.5%	30.8%	8.7%	-18.6%	6.3%
ANOVA *P* value	0.0002	0.0002	0.0502	0.0012	0.0982

Fig. 4